Analysis and Modeling of Dispersion Characteristics in AlGaN/GaN MODFETs

Shawn. S.H. Hsu[*] and Dimitris Pavlidis
Department of Electrical Engineering and Computer Science,
The University of Michigan, Ann Arbor, MI 48109-2122, USA
[*] Presently at Electrical Engineering, National Tsinghua University, Hsinchu 300, Taiwan

Abstract

The dispersion effects of transconductance (g_m) and output resistance (R_{ds}) in AlGaN/GaN MODFETs were investigated. The dispersion effects of g_m were found to be much smaller than those of R_{ds}. Devices under different biases show g_m dispersion of ~ 4% to 7%, while R_{ds} dispersion of ~ 19 % to 44% in a frequency range of 50 Hz to 100 kHz. The trapping-detrapping time constants of the dispersion effects were extracted by employing a novel distributed RC network and carrier injection current sources. The time constants estimated are in a range of ~ 1.5 μs to 1 ms.

I. Introduction

AlGaN/GaN MODFETs have demonstrated outstanding power performance and low-noise characteristics [1]-[2]. Excellent power performance of AlGaN/GaN MODFETs has been reported [1]. In addition, very low noise figures have been obtained [2]. Despite showing promising results for high-power and low-noise applications, the dispersion effects observed in AlGaN/GaN MODFETs are still an issue, which may cause reliability problems in GaN-based devices [3]-[4]. The pronounced dispersion effects in GaN-based devices may be attributed to the traps existing between different heterojunctions, the buffer layer, and the surface areas. From the modeling and circuit point of view, the dispersion effects can cause a deviation between the observed RF output power and the DC predicted values. To precisely predict device large-signal behavior, dispersion effects are essential to be included in a complete large-signal model.

In this paper, dispersion effects in AlGaN/GaN MODFETs are investigated under various bias conditions. Section II describes the device characteristics and the dispersion measurement setup. Section III shows the measured results for both transconductance and output resistance dispersion effects. Section IV presents a novel distributed equivalent circuit model to describe dispersion effects in AlGaN/GaN MODFETs. Section V discusses the extracted trapping-detrapping time constants and their bias dependences. Section VI concludes this work.

II. Device Characteristics and Measurement Setup

The AlGaN/GaN MODFETs investigated in this paper were grown on sapphire substrates. The gate length was 0.25 μm and the gate finger width was 0.1 mm for all devices. Fig. 1 shows the *I-V* characteristics for a 0.25×200 um^2 device. For two-finger devices, f_{max} can reach ~ 66 GHz under V_{GS}= -5.8 V and V_{DS}= 15 V. In addition, these devices present excellent input/output impedance and output power scalability for large periphery multi-finger devices.

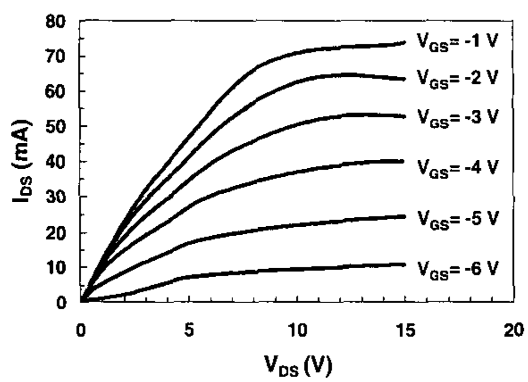

Fig. 1: *I-V* characteristics of 0.25×200 μm^2 AlGaN/GaN MODFET.

The dispersion characteristics of g_m and R_{ds} were measured using an on-wafer setup with microwave probes and coaxial cables to avoid interference and ensure accurate measurement results. The dispersion of transconductance was measured by applying a DC voltage to the drain, while an AC signal with a DC voltage offset was used for the gate bias. The dispersion effects can be extracted directly from the AC voltage across a sensing resistor (typical ~ 10 to 50 Ω) at the gate terminal. A similar setup with AC signal applied to the drain side was used for output dispersion measurements. A high-resolution sampling scope was employed to measure the voltage difference across the sensing resistor. Measurements were performed in a frequency range of 50 Hz to 100 kHz under different bias conditions.

III. Measurement Results of Dispersion Effects

The dispersion effects were observed for both g_m and R_{ds} under constant V_{DS} and constant V_{GS} conditions. Fig. 2 shows the transconductance dispersion under a fixed V_{DS} of 10 V while V_{GS} varies from -2 V to -5 V. As can be seen, the transconductance dispersion is very small over a wide range of gate voltages. Small dispersion effects were also observed for devices biased under a fixed gate voltage (-5 V) with the drain voltage changed from 5 V to 12 V. The normalized transconductance dispersion $\Delta g_m/g_m$ (where g_m is at 50 Hz, and Δg_m is the difference between 50 Hz and 100 kHz) is from ~ 4% to ~ 7% under the studied bias points.

Fig. 3 presents the output resistance dispersion under V_{DS}= 10 V and V_{GS} varies from -2 V to -5 V. As can be seen, the output resistance presents in general more obvious dispersive characteristics than the transconductance dispersion. It also can be seen that the R_{ds} dispersion increases when the gate voltage becomes more negative. For example, $\Delta R_{ds}/R_{ds}$ increases from ~ 22 % at V_{GS}= -2 V to ~ 44 % at V_{DS}= -5 V. Similar trend was also observed when V_{GS} is fixed while V_{DS} varies from 5 V to 12 V. $\Delta R_{ds}/R_{ds}$ increases from ~ 19 % at V_{DS}= 5 V to ~ 40 % at V_{DS}= 12 V.

The observed small transconductance dispersion characteristics suggest that the source resistance dispersion is small in the studied AlGaN/GaN MODFETs. Based on the simple circuit theory of source degeneration, if the source resistance depends on frequency, the external transconductance is also a function of frequency. The source resistance includes the contact resistance, the access resistance underneath the contact, and the lateral resistance between the source and the gate. In addition, the surface between the gate and the source can also contribute to the total source resistance. The observed frequency independent external transconductance indicates that the traps locating between the source and the gate do not play a dominant role on the device low-frequency dispersive characteristics.

The strong dependence of the output resistance dispersion on the bias conditions (both V_{GS} and V_{DS}) can be explained as follows: when the gate bias changes toward the pinch-off condition, the channel is beyond thermal equilibrium and free carrier injection into trapping states is enhanced. The injected charge results in an electric field, which modulates the shape of the channel leading to more pronounced frequency dependence. A similar explanation of charge redistribution and resulting electric field can be applied to the condition of fixed V_{GS} bias with V_{DS} varying from the linear to the saturation region.

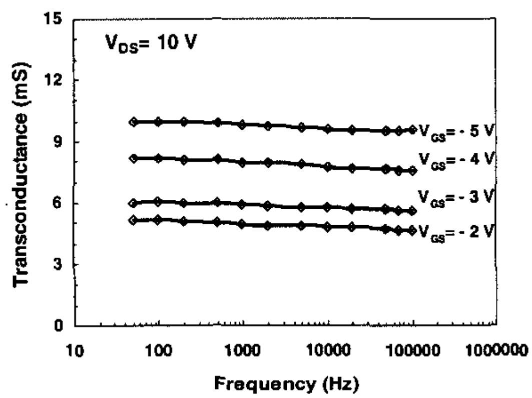

Fig. 2: Measured transconductance as a function of frequency and bias conditions for a 0.25×200 μm^2 AlGaN/GaN MODFET.

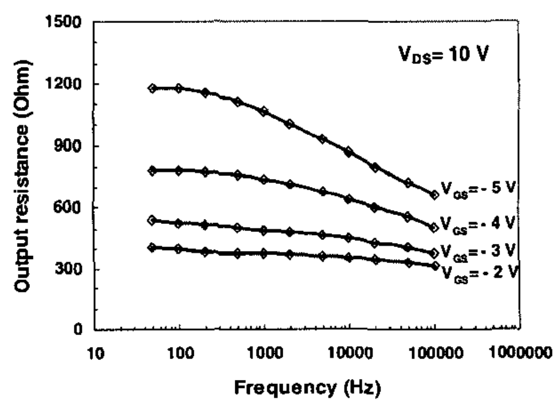

Fig. 3: Measured output resistance as a function of frequency and bias conditions for a 0.25×200 μm^2 AlGaN/GaN MODFET.

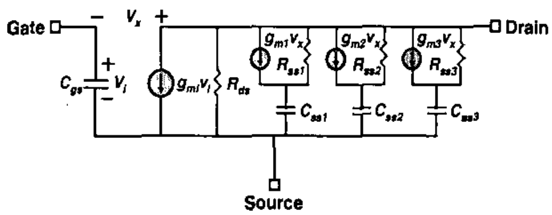

Fig. 4: Equivalent circuit model to describe dispersion effects in AlGaN/GaN MODFETs.

IV. Modeling and Analysis of Dispersion Effects

Different models have been proposed to describe dispersion effects in FETs [5]-[6]. Various equivalent circuit topologies such as resistor/capacitor network and current sources have been used to describe the observed dispersion characteristics. The model proposed in this study is shown in Fig. 4. In addition to an intrinsic FET model, multi-stage RC networks and current sources (three cells are used in this case) are employed to describe distributed trap time constants and energy states, as applicable to AlGaN/GaN MODFETs. The voltage-controlled current sources ($g_{mn}V_x$, where n= 1, 2, 3) model the degree of carrier injection into the traps, the resistances R_{ssn} describe the impedance seen by the injected carriers and the capacitances C_{ssn} model the coupling between injected carriers and their contribution to the drain-source current. In addition, it was found that the products of R_{ssn} and C_{ssn} can be used to estimate the distributed trapping-detrapping time constants.

Fig. 5 and Fig. 6 show the measured and modeled results of g_m and R_{ds} under different bias conditions. The parameters were extracted by fitting the simulated results to both the measured g_m and R_{ds} dispersion characteristics simultaneously. Excellent agreement was obtained between measured and modeled results. During the parameter extraction procedure, it was found that the carrier injection transconductance g_{mn} is insensitive to the choice of the initial values. In addition, the trapping-detrapping time constants (products of R_{ssn} and C_{ssn}) were converge to similar values in spite of using different initial values. Since the carrier injection process depends only on the trap characteristics, the associated impedances are relatively high. The values used for R_{ssn} were in the order of ~ 10^9 to 10^{11} Ω. The values of C_{ssn} were fixed as 0.1 pF (~ C_{gs}), 0.01 pF, and 0.001 pF in the optimization procedure.

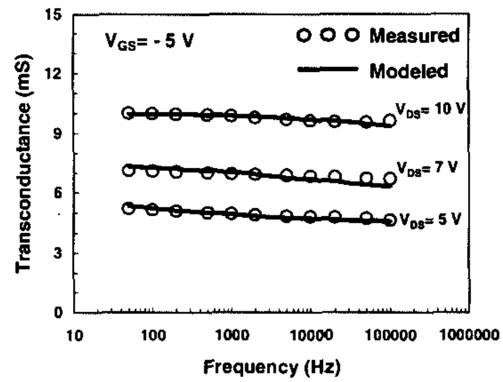

Fig. 5: Measured and modeled transconductance dispersion effects.

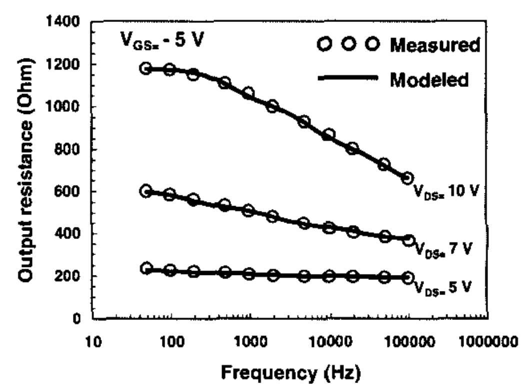

Fig. 6: Measured and modeled output resistance dispersion effects.

V. Discussion

Based on the proposed model, the trapping-detrapping time constants of the distributed RC networks can be extracted. The τ_1, τ_2, and τ_3 values are shown in Table I and Table II for constant V_{GS} and constant V_{DS} bias conditions, respectively. The time constants are distributed in three different ranges corresponding to the three RC networks necessary for best fit of the measured R_{ds} and g_m dispersion characteristics. In table I, the time constants reduce with increased V_{DS} indicating that the trapping-detrapping process occurs at a higher rate when the drain voltage increases. This may be attributed to the higher carrier energy obtained under high electric field, and consequently shorter time required for carrier injection into the traps. In addition, the reduction rate of τ becomes smaller at high V_{DS}, which may be related to saturation of the carrier energy under large electric field.

Bias (V_{GS}= -5 V) \ Tau	τ_1(s)	τ_2(s)	τ_3(s)
V_{DS}= 5 V	1.30×10^{-3}	1.21×10^{-4}	6.67×10^{-6}
V_{DS}= 7 V	8.27×10^{-4}	6.89×10^{-5}	6.23×10^{-6}
V_{DS}= 10 V	2.28×10^{-4}	2.07×10^{-5}	2.19×10^{-6}
V_{DS}= 12 V	3.01×10^{-4}	2.39×10^{-5}	2.26×10^{-6}

Table I: Extracted distributed trapping-detrapping time constants under constant V_{GS} conditions.

In table II, τ_1 shows a clear trend of time constant reduction when the device is biased toward the pinch-off condition. This may be attributed to the device operating beyond the thermal equivalent condition and therefore carriers obtaining higher energy and manifesting reduced trapping-detrapping time constants. The described trend resembles that observed under high V_{DS} bias conditions. On the other hand, the time constants τ_2 and τ_3 are less sensitive to V_{GS}.

Bias (V_{DS}= 10 V) \ Tau	τ_1(s)	τ_2(s)	τ_3(s)
V_{GS}= -2 V	6.67×10^{-4}	1.96×10^{-5}	1.69×10^{-6}
V_{GS}= -3 V	3.75×10^{-4}	1.68×10^{-5}	1.48×10^{-6}
V_{GS}= -4 V	1.96×10^{-4}	1.78×10^{-5}	1.79×10^{-6}
V_{GS}= -5 V	2.28×10^{-4}	2.08×10^{-5}	2.19×10^{-6}

Table II: Extracted distributed trapping-detrapping time constants under constant V_{DS} conditions.

VI. Conclusion

Overall, the dispersion characteristics in AlGaN/GaN MODFETs are reported and analyzed. The proposed model includes multiple RC networks with voltage-controlled current sources to describe the observed transconductance and output resistance dispersion. Excellent agreement was obtained between the measured and modeled results, which also demonstrated the suitability of using this model to precisely describe dispersion effects for devices such as AlGaN/GaN MODFETs. In addition, the dependence of extracted trapping-detrapping time constants on bias conditions was discussed. The study of the extracted parameters and their bias dependences helps identifying the physical mechanisms determining the dispersion effects in AlGaN/GaN MODFETs.

Acknowledgement: work supported by ONR (contract Nos.N00014-00-1-0879, N00014-02-1-0128) and HRL Laboratories.

[References]

[1] Y. -F. Wu, P. M. Chavarkar, M. Moore, P. Parikh, and U. K. Mishra, "Bias-dependent performance of high-power AlGaN/GaN HEMTs," *International Electron Devices Meeting, IEDM Technical Digest*, pp. 378 - 380, Washington DC, Dec. 2001.

[2] W. Lu, J. Yang, M. Asif Khan and I. Adesida, "AlGaN/GaN HEMTs on SiC with over 100 GHz f_T and low microwave noise," *IEEE Trans. Microwave Theory and Tech.*, vol. 48, No. 3, pp. 581-585, March. 2001.

[3] S. Hsu, P. Valizadeh, D. Pavlidis, J. S. Moon, M. Micovic, D. Wong, and T. Hussain, "Impact of RF stress on dispersion and power characteristics of AlGaN/GaN HEMTs," *IEEE GaAs IC Symposium*, Monterey, CA, USA, pp. 85-88, Oct. 2002.

[4] I. Daumiller, D. Theron, C. Gaquiere, A. Vescan, R. Dietrich, A. Wieszt, H. Leier, R. Vetury, U. K. Mishra, I. P. Smorchkova, N. X. Nguyen, C. Nguyen, and E. Kohn, "Current instabilities in GaN-based devices," *IEEE Electron Device Lett.*, vol. 22, no.2, pp. 62-64, Feb. 2001.

[5] J. M. Golio, M. G. Miller, G. N. Maracas, and D. A. Johnson, "Frequency-dependent electrical characteristics of GaAs MESFETs," *IEEE Trans. Electron Devices*, vol. 37, No. 5, pp. 1217-1227, May 1990.

[6] E. Kohn, I. Daumiller, P. Schmid, N. X. Nguyen, "Large signal frequency dispersion AlGaN/GaN heterostructure field effect transistors," *Electronics Lett.*, vol. 35, no.12, pp. June 1999.